Classical properties of quantum scattering

2003 J. Phys. A: Math. Gen. 36 4445

(http://iopscience.iop.org/0305-4470/36/15/316)

INSTITUTE OF PHYSICS PUBLISHING JOURNAL OF PHYSICS A: MATHEMATICAL AND GENERAL

J. Phys. A: Math. Gen. **36** (2003) 4445–4464 PII: S0305-4470(03)56834-2

Classical properties of quantum scattering

Władysław Żakowicz

Institute of Physics, Polish Academy of Sciences, Al. Lotnikow 32/46, Warsaw 02-668, Poland

Received 22 November 2002, in final form 20 February 2003
Published 3 April 2003
Online at stacks.iop.org/JPhysA/36/4445

Abstract

Quantum elastic potential scattering of a particle is re-examined taking into account exact solutions of the corresponding Schrödinger equation. In addition to the scattering of stationary plane waves and stationary finite-width wave beams, nonstationary wave packets having finite duration times are studied and some corresponding examples are presented. The role of interference between the scattered wave and the advancing incident beam is studied. Several two-dimensional scattering problems, involving axially symmetric, generic examples of nonuniform attractive and repulsive potentials, are discussed in more detail. This discussion concentrates on finding proper conditions when the solutions of the Schrödinger equation may resemble the corresponding solutions of the classical Newton equation. Examples are shown where such similarities occur.

PACS numbers: 03.65.Nk, 34.80.−i, 42.25.−p

M This article features online multimedia enhancements

1. Introduction

This paper attempts to reveal in a more explicit way the connection between the notions of scattering in classical and quantum physics.

Scattering experiments, as well as their underlying theories, are major tools allowing a microscopic investigation, description and understanding of physical systems, including e.g., atomic collisions and high energy collisions of elementary particles.

Within the frame of classical mechanics, initially free and uniformly moving along rectilinear line incident particles impinging on scatterers, or target particles, are deflected, i.e. are scattered. All those microscopic deflections of the incident particles change the average macroscopic and statistical properties of the scattered beam. Those changes, detectable experimentally, are quantitatively described by means of differential and total cross sections ($\frac{d\sigma}{d\Omega}$ and a total σ_T).

In quantum mechanics, freely moving incident particles are described by wavefunctions, usually having the form of plane waves. Due to the interaction between the incident and

the target particles (scatterers) the wavefunctions are modified and besides the incident plane wave Ψ^I (also called a primary or direct wave) one must include another wave, identified as a scattered wave Ψ^S (also called a secondary wave), propagating outwards from the scatterer.

The quantitative studies of the wavefunction in quantum scattering processes were stimulated by analogical analyses of waves scattering in many classical systems: acoustics, optics and electromagnetic waves. Quantum properties of the investigated physical systems are secured in the quantum interpretation of the wavefunction and its connection with particle measurements. Otherwise, the quantum wavefunctions and classical waves are determined by very similar equations.

Studies of classical wave scattering were initiated by Lord Rayleigh [1] discussing a disturbance (scattering) of acoustic plane waves of sound by obstacles, placed in a propagating uniform media. He found that an incident wave (primary in his terminology) induces a secondary wave (later called scattered), propagating outwards from the perturber, which had to be added to the incident wave to satisfy proper wave boundary continuity conditions. For spherically and cylindrically symmetric scatterers, Lord Rayleigh introduced 'partial waves' which have become a very convenient form to represent the scattering waves.

Researchers who followed Lord Rayleigh's analysis introduced an estimation of the effectiveness of scattering and the interaction between the incident plane wave and the perturber (which later were associated with scattering cross sections), using the magnitude of the scattered function.

In particular, this was used for the scattering of electromagnetic waves by a dielectric sphere, known as Mie scattering [2, 3] and other dielectric objects now discussed in textbooks, e.g. [4]. The same idea of scattering evaluation, by means of the magnitude of the scattered wave, has been adapted in the classical field theory to study the scattering of electromagnetic waves by a cloud of electrons [5]. In the latter case, scattered radiation has been identified with the electromagnetic radiation emitted by electrons, oscillating in the field of an incident electromagnetic wave. However, to obtain the elastic component of the forward intensity distribution, first the emitted radiation has to be superposed with the incident radiation that forced the electron oscillations. Afterwards one can determine the relevant radiation pattern.

Nowadays, quantitative evaluations of scatterings are usually expressed by means of analogical variables as in the classical case, i.e. differential and total scattering cross sections $\frac{\mathrm{d}\sigma}{\mathrm{d}\Omega}$ and σ_T.

Following the generally accepted derivation, presented in all quantum mechanical textbooks and quantum scattering treatises, and also some analogies with other wave scattering theories, the quantum scattering cross sections are expressed in terms of the scattered part of the wavefunction Ψ^S. This scattered part of the wavefunction for centrally symmetric scattering potentials $V(r)$, can be analysed in terms of partial waves, i.e. the eigenwaves of the angular momenta, and usually written with the help of the corresponding phase shifts δ_l. Thus the cross sections are written as, see e.g. [6–10],

$$\frac{\mathrm{d}\sigma(\theta)}{\mathrm{d}\theta} = \left| \frac{1}{2\mathrm{i}k} \sum_{l=0}^{\infty} (2l+1)\, \mathrm{e}^{\mathrm{i}\delta_l} \sin\delta_l P_l(\cos\theta) \right|^2 \tag{1}$$

and

$$\sigma_T = 2\pi \int_0^{\pi} \frac{\mathrm{d}\sigma(\theta)}{\mathrm{d}\theta} \sin\theta \,\mathrm{d}\theta = \frac{4\pi}{k^2} \sum_{l=0}^{\infty} (2l+1) \sin^2\delta_l. \tag{2}$$

A precise description of quantum scattering has been formulated using mathematical methods of Hilbert space and functional analysis, see e.g. [11, 12]. In this language, the scattering is often defined as a transition between asymptotically free states at the remote past ($t \to -\infty$)

and distant future ($t \to +\infty$) realized by the relevant evolution wave operators. Adapting this sophisticated precise mathematical formulation of the scattering to its physically measurable description leads to similar expressions for the differential and total cross sections as are given by equations (1) and (2).

However, deriving these expressions, Schiff had already noted that, according to the strict principles of quantum mechanics, the particle density and current, given by quadratic expressions of the wavefunction, should include the interference terms between Ψ^S and Ψ^I, when these parts of the wavefunction overlap. Nevertheless, he believed that with the help of additional collimators the incident and the detected scattered beams can be separated, thus justifying the above treatment. However, not dismissing his expectation, we point out that those collimators would introduce other scattering elements. Their effect would be difficult to distinguish from the true scattering caused by the target particles. Without adding any external collimators, the quantum analysis of scattering can be done in a more consistent manner if the infinitely extended incident plane waves are replaced by wave beams having finite transverse cross sections and finite lengths (duration time). In fact, only such beams occur in scattering experiments.

As had been noted by Newton [8] the use of monochromatic incident waves would produce convergence difficulties in scattering theories. For mathematical reasons, the scattering waves should be replaced by wave packets. In the following, it is shown how finite wave packets can be incorporated into the scattering theory in a quantitative way. Verifying equations (1) and (2), as well as establishing their range of validity, let us generalize the discussion of scattering by taking into account the finite dimension of beams; in section 2 for stationary beams having finite transverse dimensions but infinitely extended along their length, and in section 3 we will consider finite duration of pulses, also describing their time evolution.

Attempting quantitative studies of scattering, which take into account the finite cross sections of incident beams, let us simplify our analysis considering this problem in two spatial dimensions. This simplification is not very crucial in the treatment of the plane wave scattering, however, a description of finite-dimensional beams is much easier on a two-dimensional plane than in three-dimensional space. That is due to the much simpler form of the angular components of the partial waves; $e^{in\phi}$ in the first case and spherical harmonics $Y_{lm}(\theta, \phi)$ in the second one. In addition, graphical presentations of the obtained results are much easier.

A finite-width wavefunction in scattering problems can be obtained by a superposition of an appropriate bundle of the scattering wavefunctions. The wavefunctions forming this bundle include the plane waves propagating within the accordingly selected angular sector.

Though our discussion is restricted to 2D models, this approach may be valid for almost any regular, finite-range axially symmetric interaction potential $V(r)$. It requires building, for a chosen $V(r)$, a library of special functions being solutions of the radial Schrödinger equations in the internal region. These libraries can be built using standard numerical procedures and solving a set of ordinary differential equations. An illustration of these functions is presented in the appendix.

Our particular examples correspond to a finite range of attractive ($V_0 < 0$) and repulsive ($V_0 > 0$) interaction potentials of the form

$$V(r) = \begin{cases} V_0 \left(\frac{r}{a} - 1\right)^2 & r \leqslant a \\ 0 & r > a. \end{cases} \tag{3}$$

Throughout this paper, the Schrödinger equation is used in the dimensionless form

$$\nabla_{\mathbf{r}}^2 \Psi_E(\mathbf{r}) + 2(E - V(r))\Psi_E(\mathbf{r}) = 0 \tag{4}$$

in which the particle energies and the interaction potentials are measured in unit of E_0 (typical for the selected problems), the unit of length is $l_0 = \hbar/\sqrt{mE_0} = \lambda_B/(\sqrt{2}\pi)$, where λ_B is the de Broglie wavelength for the selected energy E_0, and the times t are given in $\hbar/E_0$.

2. Quantum scattering—stationary states

2.1. Plane wave scattering

A solution of the stationary Schrödinger equation for a particle in the presence of a perturbing potential $V(r)$ corresponding to the incident plane wave propagating in the direction $\mathbf{k}(\alpha) = k\{\cos\alpha, \sin\alpha, 0\}$, $k = \sqrt{2E}$, can be looked for using partial wave expansion

$$\Psi_{\mathbf{k}}(x, y) = \begin{cases} \mathrm{e}^{\mathrm{i}\mathbf{k}(\alpha)\cdot\mathbf{r}} + \sum_{n=-\infty}^{\infty} c_n H_n^{(1)}(kr)\,\mathrm{e}^{\mathrm{i}n(\phi-\alpha)} & r > a \\ \sum_{n=-\infty}^{\infty} a_n \psi_{kn}(r)\,\mathrm{e}^{\mathrm{i}n(\phi-\alpha)} & r < a \end{cases} \tag{5}$$

where $H_n^{(1)}\,\mathrm{e}^{\mathrm{i}n\phi}$ are propagating outward partial wave solutions of the stationary Schrödinger equation outside the scatterer represented by V, and ψ_{kn} represent the corresponding regular solutions in the internal region, $r \leqslant a$. These internal solutions can be found solving the equation

$$\frac{\mathrm{d}^2}{\mathrm{d}r^2}\psi_{kn} + \frac{\mathrm{d}}{r\,\mathrm{d}r}\psi_{kn} + (k^2 - 2V_{\mathrm{eff}}(n, r))\psi_{kn} = 0 \tag{6}$$

where

$$V_{\mathrm{eff}}(n, r) = V(r) + \frac{n^2}{2r^2}. \tag{7}$$

When $V(r) = \textit{constant}$, these solutions can be explicitly written in terms of the Bessel functions J_n or I_n. In the general cases they can be determined numerically, starting from the initial data at points inside the centrifugal barrier close to $r = 0$.

For $V(r)$ regular in the vicinity of the centre, equation (6) reduces to the Bessel equation and the initial data for the internal partial wavefunctions can be taken according to

$$\psi_{kn}(r \sim 0) \simeq \begin{cases} J_n\big(r\sqrt{k^2 - 2V(0)}\big) & (r \sim 0) \qquad k^2 > 2V(0) \\ I_n\big(r\sqrt{2V(0) - k^2}\big) & (r \sim 0) \qquad k^2 < 2V(0). \end{cases} \tag{8}$$

These internal wavefunctions do not have to be normalized, as the proper normalization of the total wavefunctions will be secured if the continuity conditions for Ψ and Ψ' at $r = a$ are fulfilled. These boundary conditions provide

$$a_n = \frac{\mathrm{i}^n k}{W_n}\big(J_n(ka)H_n^{(1)\prime}(ka) - J_n'(ka)H_n^{(1)}(ka)\big) \tag{9}$$

$$c_n = \frac{\mathrm{i}^n}{W_n}(J_n(ka)\psi_{kn}'(a) - kJ_n'(ka)\psi_{kn}(a)) \tag{10}$$

where

$$W_n = \big(\psi_{kn}'(a)H_n^{(1)}(ka) - k\psi_{kn}(a)H_n^{(1)\prime}(ka)\big). \tag{11}$$

The first solutions of this type were obtained by Lord Rayleigh [1] for the sound waves propagating in a homogeneous media and perturbed by a small uniform cylindrical obstacle.

In the scattering theories the total wavefunction, Ψ^T, is customarily written as a sum of the incident wave, Ψ^I (also called a 'primary wave'), satisfying the free wave equation, and its modification known as the scattered wave, Ψ^S (or 'secondary wave' in older discussions),

$$\Psi_{\mathbf{k}}^{T} = \Psi_{\mathbf{k}}^{I} + \Psi_{\mathbf{k}}^{S}. \tag{12}$$

The scattered wave $\Psi_{\mathbf{k}}^{S}$ includes the cylindrical waves propagating outwards from the scatterer. Most of the quantitative estimations of the scattering process, in particular the flux of scattered particles and the differential and total scattering cross sections, are calculated employing the scattered (or secondary) wave $\Psi_{\mathbf{k}}^{S}$ only. Thus in the asymptotic region ($r \gg a$) one has for a particle incident along the x-axis,

$$\Psi^{S}(r,\phi) \sim \frac{f(kr,\phi)}{\sqrt{kr}} = \sqrt{\frac{2}{\mathrm{i}\pi kr}}\,\mathrm{e}^{\mathrm{i}kr} \sum_{n=-\infty}^{\infty} c_n \mathrm{i}^{-n}\,\mathrm{e}^{\mathrm{i}n\phi} \tag{13}$$

leading to the differential cross section,

$$\left(\frac{\mathrm{d}\sigma}{\mathrm{d}\phi}\right)(\phi) \propto |f(kr,\phi)|^2 \propto \left|\sum_{n=-\infty}^{\infty} c_n \mathrm{i}^{-n}\,\mathrm{e}^{\mathrm{i}n\phi}\right|^2 \tag{14}$$

and for the total scattering cross section, because of the orthogonality of the different partial cylindrical waves, one obtains

$$\sigma_0 = \int_{-\pi}^{\pi} \left(\frac{\mathrm{d}\sigma}{\mathrm{d}\phi}\right) \mathrm{d}\phi \propto \sum_{n=-\infty}^{\infty} |c_n|^2. \tag{15}$$

Similar formulae for a radially symmetric interaction in three dimensions, expressed by means of partial phase shifts, are given in all textbooks and monographs on quantum mechanics and scattering. However, the scattered wave Ψ^S is only one constituent of the quantum wavefunction (or the total wave in the classical wave theories). It is not certain whether the probabilistic interpretation of the wavefunction in quantum mechanics can be extended to parts of the wavefunctions. Schiff in [6] pointed out that, with a strict application of quantum mechanical rules in the computation of particle densities and currents, there should be interference terms between the incident and scattered waves. It was expected that in real experiments such interferences should not be important. In all such experiments, the incident and scattered waves are intentionally separated with the help of applied additional collimators properly shaping the particle beams. These interferences were only important in the forward scattering and incorporated in establishing both the form and the properties of an optical theorem. The optical theorem relates the imaginary part of Ψ^S in the forward direction, $\phi = 0$, with the total cross section.

The scattering of a particle represented by a plane wave by attractive ($V_0 < 0$) and repulsive ($V_0 > 0$) potentials of the form given by equation (3) is illustrated in figures 1 and 2. These figures show the magnitudes of $\left|\Psi_{\mathbf{k}}^{I}(x,y)\right|$, $\left|\Psi_{\mathbf{k}}^{S}(x,y)\right|$ and $\left|\Psi_{\mathbf{k}}^{T}(x,y)\right|$ for the plane wave incident along the x-axis. Some radial internal partial waves $\psi_k(n,r)$, used in these calculations, are presented in the appendix.

As it is seen, the incident plane waves are represented by not very interesting uniform particle densities. The scattered parts of the wavefunctions Ψ^S are mostly concentrated in the forward direction with much weaker waves at adjacent directions in the forward sector. A similar enhanced forward scattering has been recognized as a nonclassical feature of the quantum scattering [7].

However, just behind the scatterer, where the scattered wavefunctions show such a profound concentration, the total wavefunctions Ψ^T show dips in the particle densities, clearly visible as shadows (particularly in the case of the repulsive blocking potential). In a similar manner we speak about a shadow scattering [8].

Only the data derived for the complete wavefunction, i.e. either Ψ^I being the true wavefunction in the absence of any perturber, or Ψ^T being a true wavefunction in the presence

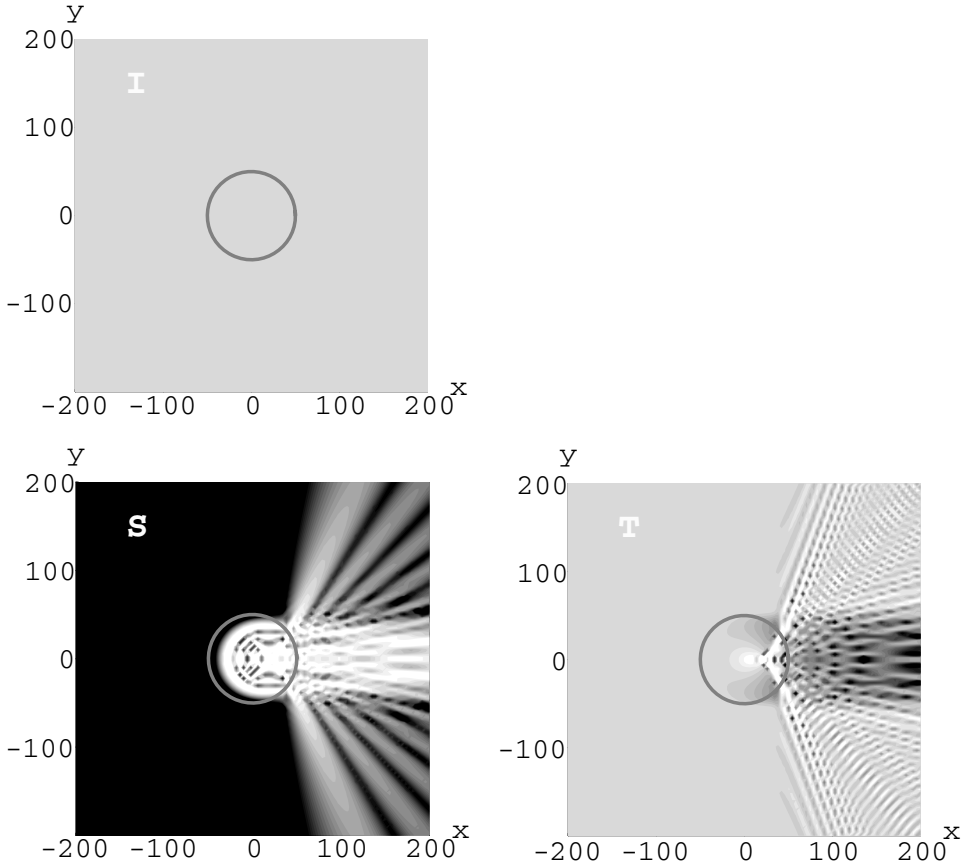

Figure 1. Magnitudes of an incident plane wavefunction for a particle incident along the x-axis (I), the scattered part of a wavefunction (S) and the total wavefunction (T), with a scatterer at the centre, attractive interaction (particle energy $E = 1$, $V_0 = -3$ and $a = 50$).

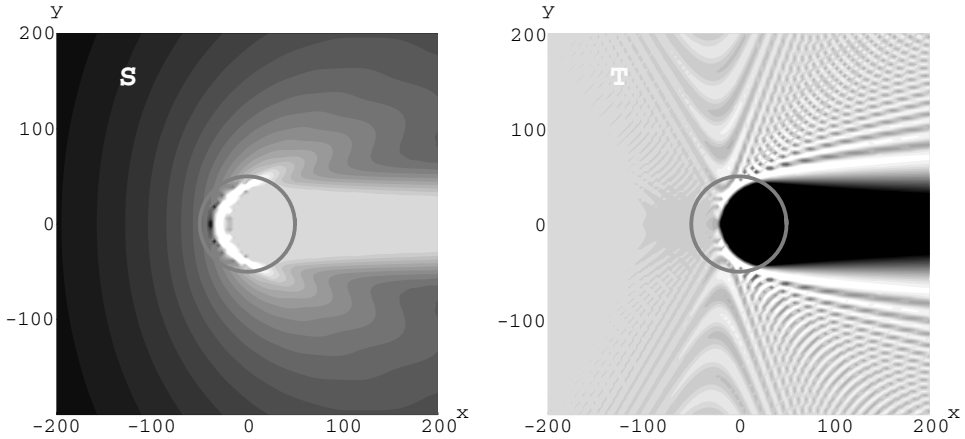

Figure 2. Scattered part of wavefunction (S) and total wavefunction (T), with a scatterer at the centre, (for repulsive interaction ($V_0 = 3$, $E = 1$ and $a = 50$).

of a perturber may be interpreted in terms of the particle densities and currents; Ψ^S being a part of the wavefunction, in those regions where it overlaps with Ψ^I, should not be interpreted in particle terms. Thus, for the incident plane waves, uniformly extending over the whole space, Ψ^S should nowhere be treated as a true wavefunction.

There would be no restrictions on these statements if only plane small ($\ll\lambda_B$) particle detectors, insensitive to wave coherences, were used. More general detective schemes, which sometime are able to distinguish between contributions from Ψ^S and Ψ^I, are briefly commented on in the final section.

To formulate a more consistent theory of scattering, the incident plane waves should be replaced by particle beams. In the next subsection this problem is investigated in more detail.

2.2. Finite transverse width wave beam scattering

The importance of the analysis of finite cross section incident beams has been noted in most monographs on quantum scattering. However, finding that for weakly divergent, and in consequence broad, incident beams the phase shifts are not much different from those found for the plane waves, the quantitative analyses are often reduced to qualitative ones.

Our discussion of beam scattering will be given in quantitative terms. The introduction of the finite cross section beams is particularly simple due to the linearity of the Schrödinger equation. Superposing the solutions given by equation (5) for various angles α, with additional weights and position-dependent phase shifts, one may describe a large class of beams having arbitrary positions and orientations with respect to the scatterer.

Thus, when the incident plane wave $\mathrm{e}^{\mathrm{i}\,\mathbf{k}\cdot\mathbf{r}}$ is replaced by

$$\mathrm{e}^{\mathrm{i}\,\mathbf{k}(\alpha)\cdot\mathbf{r}} \longrightarrow \langle \mathrm{e}^{\mathrm{i}\,\mathbf{k}(\alpha)\cdot(\mathbf{r}-\mathbf{r_0})}\rangle_P = \int_{-\pi}^{\pi} P(\alpha)\,\mathrm{e}^{\mathrm{i}\,\mathbf{k}(\alpha)\cdot(\mathbf{r}-\mathbf{r_0})}\,\mathrm{d}\alpha \tag{16}$$

the corresponding factors $\mathrm{e}^{\mathrm{i}n\alpha}$ multiplying the expansion coefficients $\{a_n, c_n\}$ have to be replaced by

$$\mathrm{e}^{\mathrm{i}n\alpha} \longrightarrow \langle \mathrm{e}^{\mathrm{i}n\alpha}\,\mathrm{e}^{-\mathrm{i}\,\mathbf{k}(\alpha)\cdot\mathbf{r_0}}\rangle_P = \int_{-\pi}^{\pi} \mathrm{e}^{\mathrm{i}n\alpha} P(\alpha)\,\mathrm{e}^{-\mathrm{i}\,\mathbf{k}(\alpha)\cdot\mathbf{r_0}}\,\mathrm{d}\alpha. \tag{17}$$

Choosing a Gaussian amplitude function $P(\alpha) = (w/\sqrt{\pi})\,\mathrm{e}^{-w^2\alpha^2}$, where w specifies the beam width at the position of its waist $\mathbf{r_0}$, and the beam angular spread $\Delta = 1/w$. Assuming that $\Delta \ll 1$ one may approximate $\mathbf{k}(\alpha) \approx k\{1-\alpha^2/2, \alpha, 0\}$. Finally, the following approximations for a finite profile incident beam [13, 14],

$$\Psi_k^{\mathrm{inc}}(x, y) \approx \frac{2w}{\sqrt{4w^2 + 2\mathrm{i}k(x - x_0)}}\,\mathrm{e}^{\mathrm{i}k(x-x_0)} \exp\left(-\frac{k^2(y - y_0)^2}{4w^2 + 2\mathrm{i}k(x - x_0)}\right) \tag{18}$$

and multiplying factors $\langle \mathrm{e}^{\mathrm{i}n\alpha}\,\mathrm{e}^{-\mathrm{i}\,\mathbf{k}(\alpha)\cdot\mathbf{r_0}}\rangle_P$

$$G_{n,w,\mathbf{r_0}} = \langle \mathrm{e}^{\mathrm{i}n\alpha}\,\mathrm{e}^{-\mathrm{i}\,\mathbf{k}(\alpha)\cdot\mathbf{r_0}}\rangle_{w,x_0,y_0} \approx \frac{2w}{\sqrt{4w^2 - 2\mathrm{i}kx_0}}\,\mathrm{e}^{-\mathrm{i}kx_0} \exp\left(-\frac{(n + ky_0)^2}{4w^2 - 2\mathrm{i}kx_0}\right) \tag{19}$$

can be found. Using the above expressions, one can describe the wave beams of a given width w (or spread Δ) and concentrated at an arbitrary point $\mathbf{r_0} = \{x_0, y_0\}$, incident along the x-axis and scattered by a cylindrically symmetric potential $V(r)$. Note that the beam displacement, in the direction of the y-axis, measured by y_0, may play an analogous role to the impact parameter in classical scattering. Examples of the partial wave expansion coefficients, and their transformation for finite-width beams, are shown in figure 15 (see the appendix).

The corresponding beam scattering stationary wavefunction, parametrized by the energy $E = k^2/2$, the beam width w and the incident beam waist position $\mathbf{r_0}$, is denoted as $\Psi^T_{E,w,\mathbf{r_0}}(\mathbf{r})$.

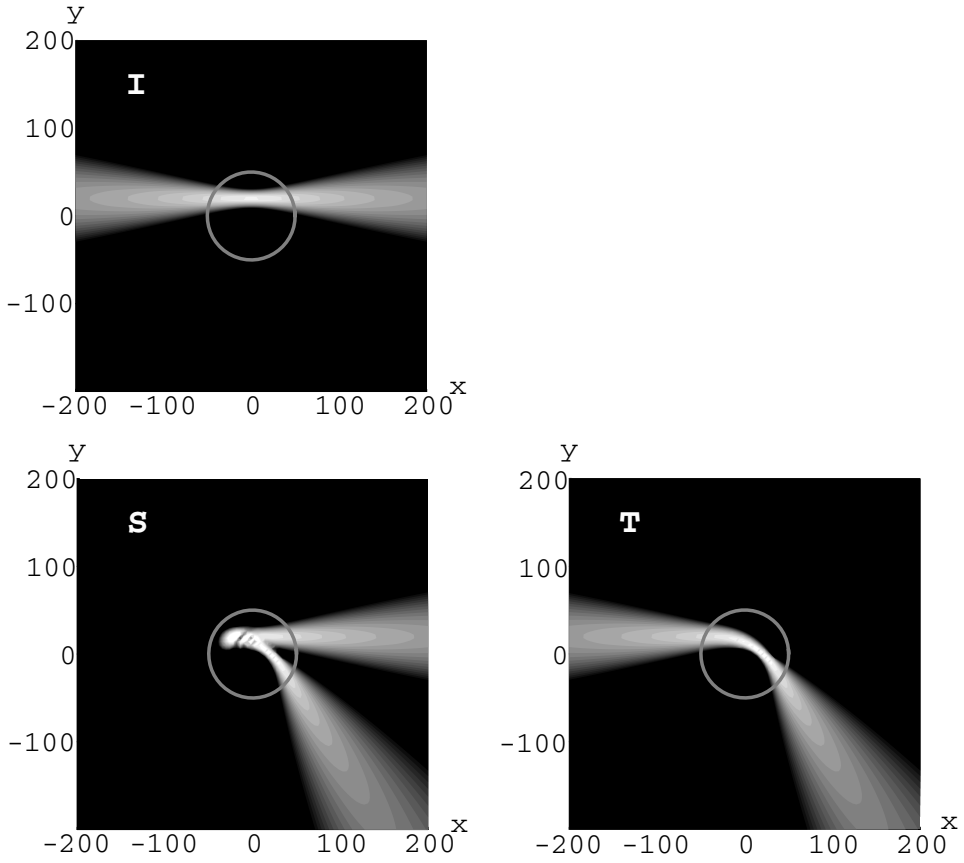

Figure 3. Incident narrow beam wavefunction (I), scattered part of wavefunction (S) and total wavefunction (T); the same attractive scatterer as in figure 1, the beam width $w = 5$, the beam is shifted to $y_0 = 20$ and concentrated at $x_0 = 0$ plane.

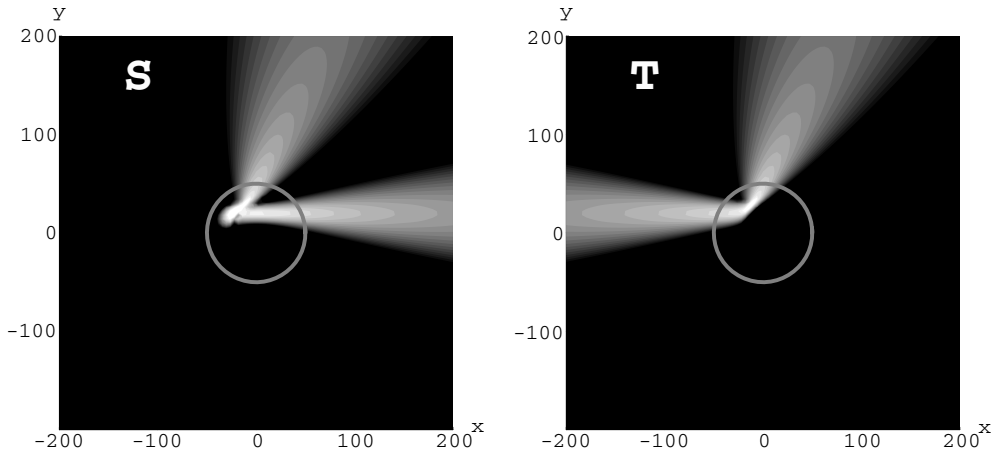

Figure 4. Scattered part of wavefunction (S) and total wavefunction (T); the same repulsive scatterer as in figure 2 and the same incident beam as in figure 3.

The free beams may stay transversally concentrated within limited intervals along their length. The length of these intervals decreases for more confined and therefore more divergent beams, (i.e. when $w \searrow 0$). Beyond the confinement intervals the beams spread indefinitely. Such beams in the confinement regions, before collision with a perturber, show properties analogous to free classical rectilinear motions represented by straight orbits or paths. A perturbation of the free beam by a scatterer causes changes in its free motion. All such changes are summarized as a scattering. The above notion of scattering is the same in both classical and quantum physics.

Keeping the above analogy between classical paths and quantum beams, one may investigate similarities and differences between classical and quantum scattering.

Note that the quantum beams, being two-dimensional objects, are characterized by more parameters than the corresponding one-dimensional classical trajectories. In addition to the displacement y_0, which can be treated similarly as the impact parameter of a scattered classical particle, one can include the beam width w and the position of its maximum concentration x_0.

Figures 3 and 4 show scattering of narrow beams ($w = 5 \ll a = 50$) by two scattering attractive ($V_0 = -3$) and repulsive ($V_0 = 3$) potentials. The beams, incident along the x-axis, are concentrated in the plane perpendicular to the x-axis, passing through the centre of a scattering atom ($x_0 = 0$). The properties of the incident beams are completely specified by Ψ^I, being the true quantum mechanical wavefunctions in the absence of any scatterer.

As these pictures show, in both attractive and repulsive cases, there are two beams derived using the scattered wave Ψ^S only, and propagating outwards from the scatterer. While one of them, in each case, represents a deflected function, the second coincides with the incident beam. However, according to the widely accepted definitions in scattering theories, they should be considered as scattered beams. This 'summed scattered flux' based on Ψ^S would be twice as large as the flux of the incident particles. These difficulties can be resolved noting that the corresponding superpositions of the scattered parts of the wavefunctions Ψ^S cannot provide the correct densities or currents of the scattered particles along the path of the incident wave.

In contrast to the above 'scattered beams' the beam density distributions determined using the total wavefunction Ψ^T show only the deflected parts of the beams. These distributions, corresponding to the appropriate narrow bundles inside the interaction region, have the form of single entities which look similar to the deflected orbits in classical motion. The wave-like or quantum features of these beams are manifested in their shrinking when approaching (and spreading when departing from) the position of maximum concentration.

When, in the region of significant interaction, the scattering wavefunctions are not so narrow, then, upon passing the scatterer, these wavefunctions split into several smaller beams. That happens, for example, when the incident beam is focused not inside the scatterer but at a large distance before it. This distance must be sufficiently large, so that, due to natural spreading of the concentrated beam in free motion, the beam entering the interaction region becomes broad. In consequence, the incident beam splits into multiple sub-beams, as illustrated in figures 5 and 6. The above splitting of the incident beams into separated pieces, which appear in detecting devices as separated intensity peaks, is the most evident demonstration of wave and quantum properties of matter in the scattering process. These pictures also illustrate why Young, and earlier Grimaldi, demonstrating interference effects had to use the sun's light first transmitted through a small opening [15].

Generalizing the discussion of scattering from a homogeneous cylinder [14], one may point out that scattering processes modify the incident beam in two ways. Firstly, some fraction of the incident beam is deflected (scattered) out of the beam, and may be experimentally measured by detectors surrounding the incident beam but placed outside this beam. The

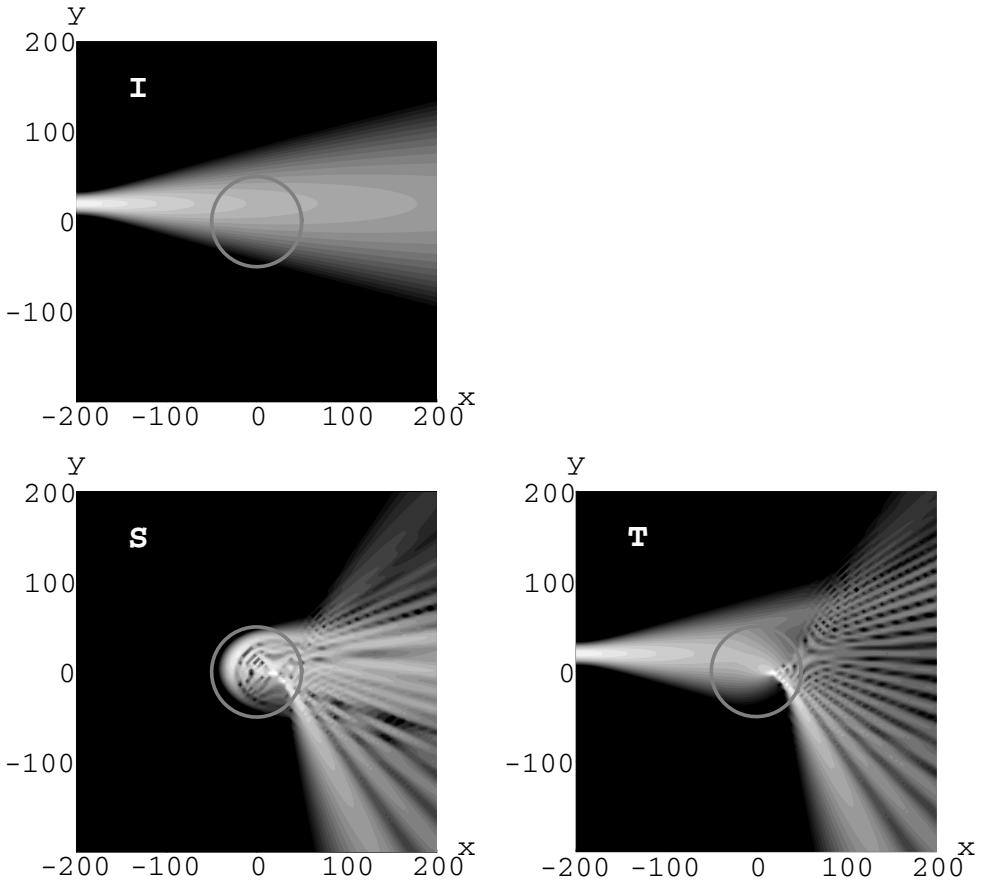

Figure 5. The same situation as in figure 3, except that the incident beam waist is shifted to the $x_0 = -200$ plane.

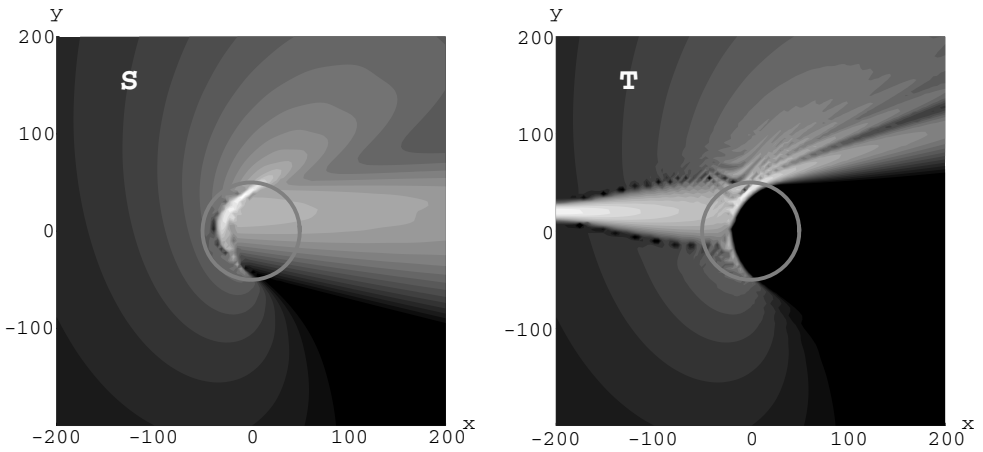

Figure 6. The same situation as in figure 4, except that the incident beam waist is shifted to the $x_0 = -200$ plane.

evaluation of this scattering can be done using the scattered part of the wavefunction Ψ^S, and expressions for the differential cross section $\frac{d\sigma}{d\phi}$ kept beyond certain small forward and backward angles ϕ_B specified by the incident beam (and dependent on the distance from the scatterer and the actual beam width). Secondly, the scattering by removing some parts of the beam modifies the incident beam itself, i.e. within the forward sector $-\phi_B < \phi < \phi_B$. The estimation of this modification cannot be given using Ψ^S, instead the two experiments and fluxes have to be compared; the first experiment, performed with the scatterer present, and described by the complete wavefunction Ψ^T, and the second one, being a reference experiment, done with the same incident beam in the absence of the scatterer, and described by Ψ^I.

Both modifications, i.e. outside and inside the incident beam, are not independent, as they are the result of the same scattering process. Their connection is referred to as an optical theorem and for incident plane waves discussed in most textbooks on quantum mechanics. An illustration of the optical theorem for finite-width beam scattering by hard cylinders is given in [14].

Figures 7 and 8 present the intensities of the forward scattering for non-centrally incident beams, wider than the range of attractive/repulsive interaction, at several distances (exponentially increasing) from the scatterer. At small distances, there are characteristic shadows just behind the scatterer, accompanied by very rapid intensity oscillations around the incident beam intensity (plotted as a dotted line) in those parts of the incident beams which geometrically pass outside the scatterer. Such oscillations are sometimes interpreted as caused by sharp edge diffraction, however, our 'scatterer edges' are rather smooth. Behind the scatterer, inside the shadow region, one can find a distinct 'scattering intensity distribution' computed using the scattered part of the wavefunction Ψ^S. Sometime these parts are treated as evidence of either quantum scattering, e.g. [7], or wave scattering, e.g. [4]. However, these distributions cannot be detected in any direct measurements.

Increasing the distance from the scatterer, the number of intensity modulations decreases and eventually they disappear, being moved outside the beam. At the same time, the shadow behind the scatterer disappears, being gradually filled with penetrating wavefunctions. At very large distances, this wavefunction of the scattered beam becomes very similar in its shape to the shape of the freely propagating and spreading incident beam. However, it is diminished in its amplitude as some fraction of the incident beam has been scattered outside.

Because of the optical theorem for beams, one can measure either the total integrated flux of scattered particles out of the beam, or the difference between the incident flux in the absence of a scatterer (thus determined by Ψ^I) and the true particle flux with a scatterer present (determined by Ψ^T) integrated across the transverse cross section of the incident beam.

The scattered fluxes determined both ways are equal. However, they are functions of the separation of detectors from the scatterer. These values become fixed at the distances where all intensity fringes within the incident beam disappear, and a similarity between the scattered and incident fluxes is reached.

The value of this asymptotic distance R_{asy} depends on the width of the incident beam w, and on the properties of the scatterer, e.g. the range of the interaction a, or on the value of the total cross section σ_T which is being determined. For increasing incident beam width w, the asymptotic distances R_{asy} grow, while the difference between the fluxes with and without the scatterer decreases. Thus the measurements of the forward asymptotic fluxes require higher and higher precision detectors. This shows that the use of the optical theorem in determination of the total elastic scattering cross section may be difficult.

It is remarkable that at larger distances the forward scattering patterns, for the corresponding attractive and repulsive potentials, are very similar.

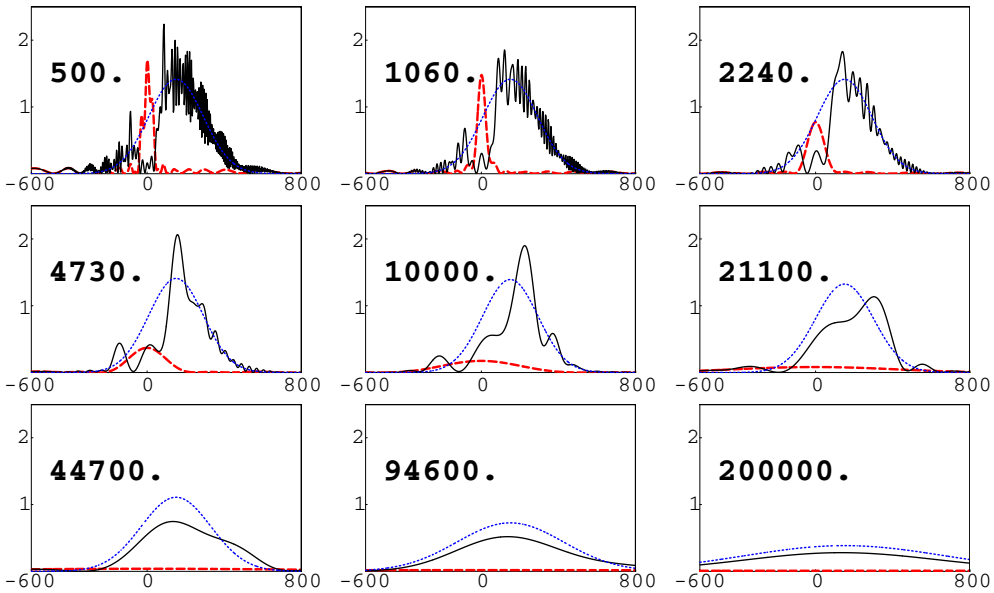

Figure 7. Forward scattering patterns illustrating the magnitudes of Ψ^I (dotted line), Ψ^S (dashed line) and Ψ^T (solid line), in the case of an attractive interaction, for a wide non-central incident beam at increasing distances from the scatterer ($V_0 = -3, a = 50, E = 1, w = 200, y_0 = 150, x_0 = 0$).

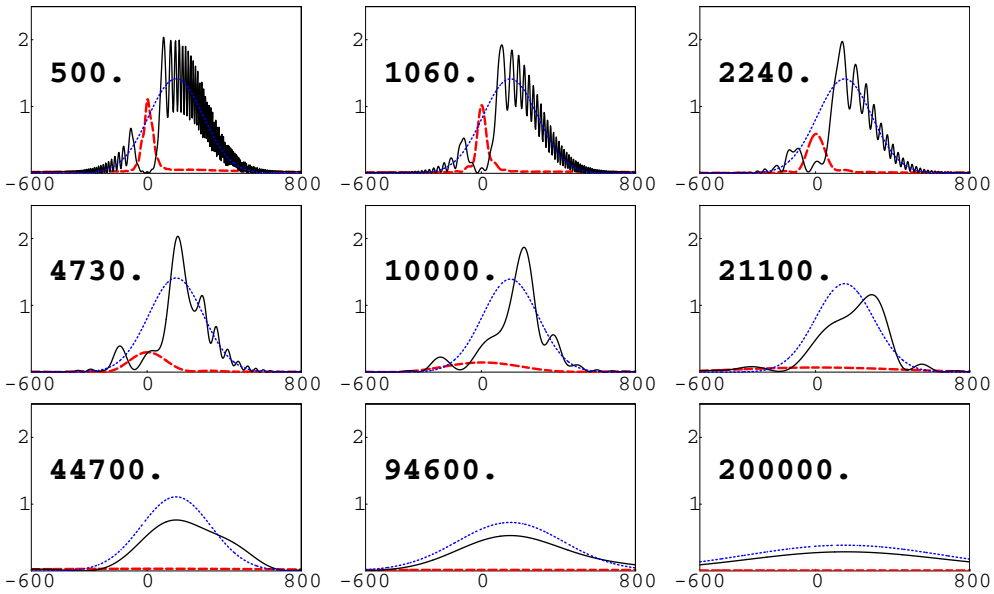

Figure 8. The same as in figure 7, but for a repulsive interaction ($V_0 = -3$).

3. Quantum scattering—time dependence

Although some causal relations between the incident and scattered states are expected, and, in fact, scattering is described in terms of time events, such an interpretation is not very

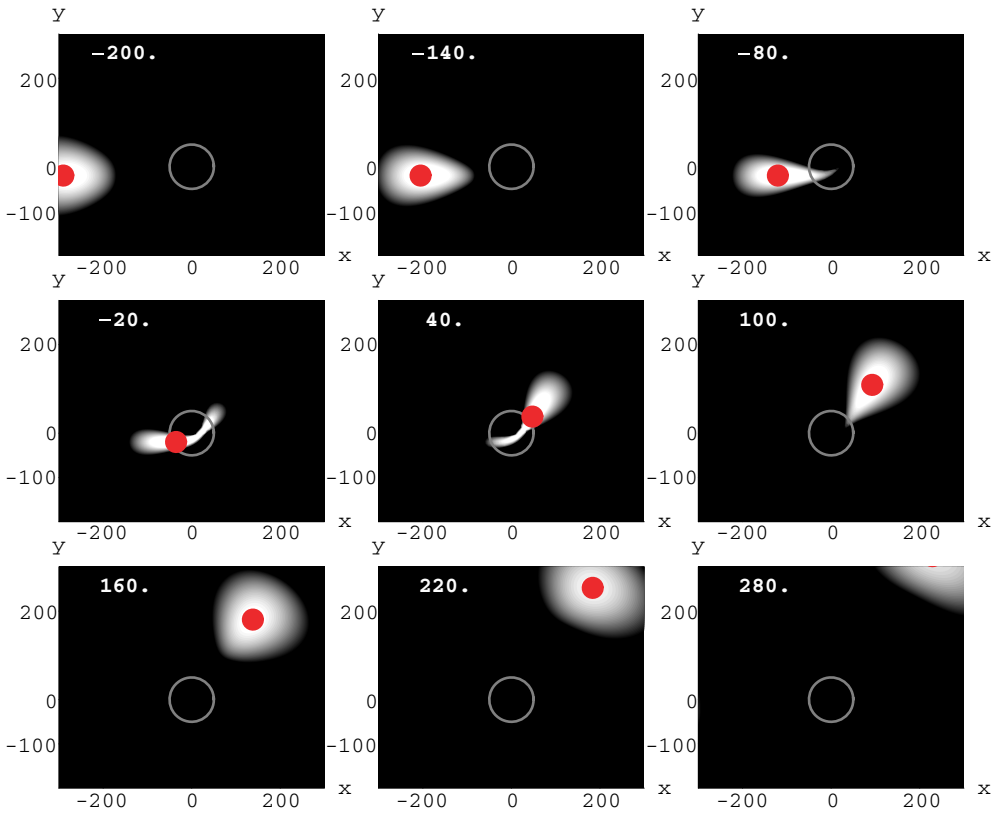

Figure 9. Evolution of finite duration time, moderately narrow wave packets, concentrated in the $x_0 = 0$ plane, composed of eigen-energy wavefunctions similar to that presented in figure 3. It is attractively interacting with a central scatterer, shown as a function of time according to the Schrödinger equation ($V_0 = -3$, $\Delta E = 0.05$, $\delta E = 0.04$). The discs placed in the centre of the wave packets represent a classical particle moving according to Newton's equation. This wave packet exhibits the classical features of a comet-like motion.

consistent with the stationary picture of scattering used in the previous section. Using the stationary states, the particle densities and currents are of course not time dependent, and only the space dependence of the scattering beams is determined. This is like the shape and positions of classical particle paths, or orbits.

Nonstationary states, corresponding to the scattering of a finite duration time incident pulse, can be constructed by a superposition of the stationary scattering wavefunctions just described, corresponding to selected sets of their energies $\{E_1, E_2, \ldots\}$ and their amplitudes $\{g_1, g_2, \ldots\}$,

$$\Psi^T(\mathbf{r}, t) = \sum_{j=1} g_j \, \mathrm{e}^{\mathrm{i}E_j t} \Psi^T_{E_j}(\mathbf{r}). \tag{20}$$

Actually, the energy spectrum for the scattered states is continuous, and to describe the solution of an arbitrary initial problem, this discrete sum should be replaced by an integral over the continuous variable E and amplitude functions $g(E)$. The above discrete formulae should be treated as samples of the general expressions. They are not supposed to provide solutions for an arbitrary initial problem of the time-dependent Schrödinger equation, but, as is demonstrated, can illustrate properties of a rich class of those solutions.

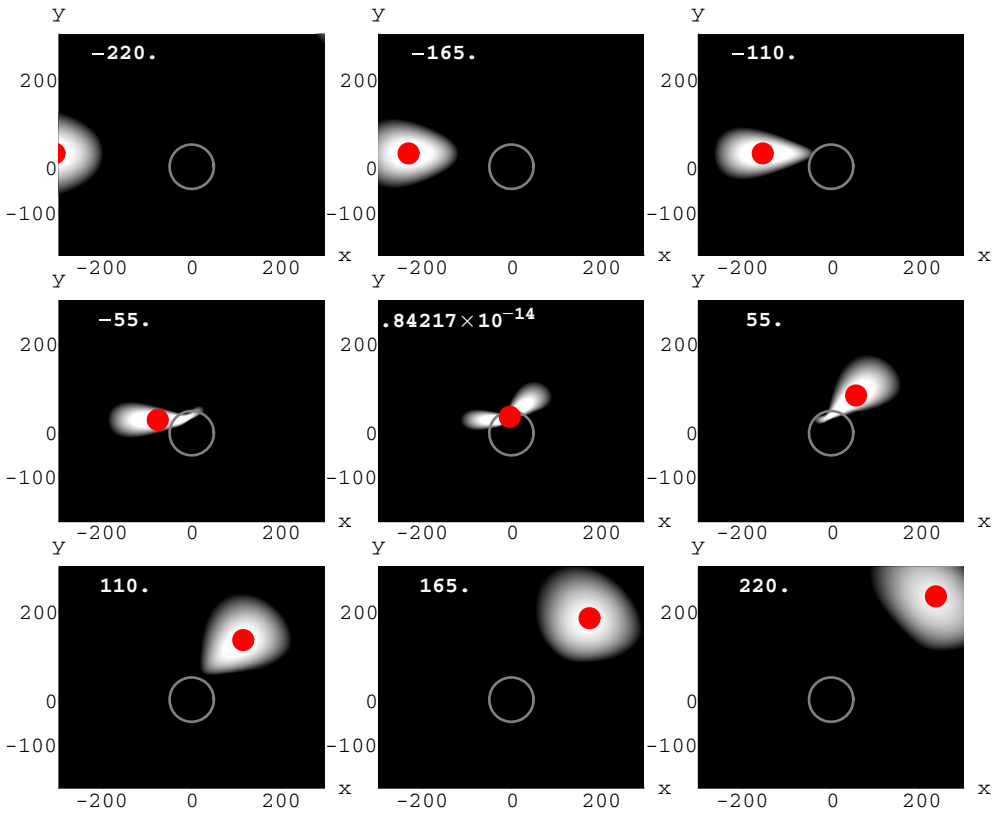

Figure 10. The same as in figure 9 for a repulsive interaction ($V_0 = 3$). The wave packet exhibits the classical features of a billiard-bowl collision.

Selecting the stationary finite-width beams described in the previous section and specified by the parameters w and $\mathbf{r_0}$, one can build, according to equation (20), nonstationary wave packets composed of those stationary wavefunctions with the same width and shifts.

We select the sampling set of energies to correspond to the equally spaced energies in an interval ΔE, centred around a mean value E_0,

$$E_j = E_0 + j\frac{\Delta E}{2N} \qquad j = 0, \pm 1, \ldots, \pm N.$$

The amplitudes g_j will be taken according to a Gaussian function

$$g(E) = \mathcal{N} \exp\left(-\frac{(E - E_0)^2}{\delta E^2}\right)$$

where the width of this Gaussian δE is of the order of ΔE.

Sampling the energies at a set of finite values one obtains the wavefunctions being periodic in time. Selecting a sufficient number of terms E_j, it is possible to find that in a given time and space interval $\Delta T \times \Delta \mathbf{R}$ only one wave packet is visible, thus approximating the evolution of a single confined particle.

Figures 9–13 show time evolutions of finite space and duration time pulses scattered by attractive and repulsive potentials specified previously. The same pulse evolution is shown in video films 1–4 (multimedia movies are available from the article's abstract page in the

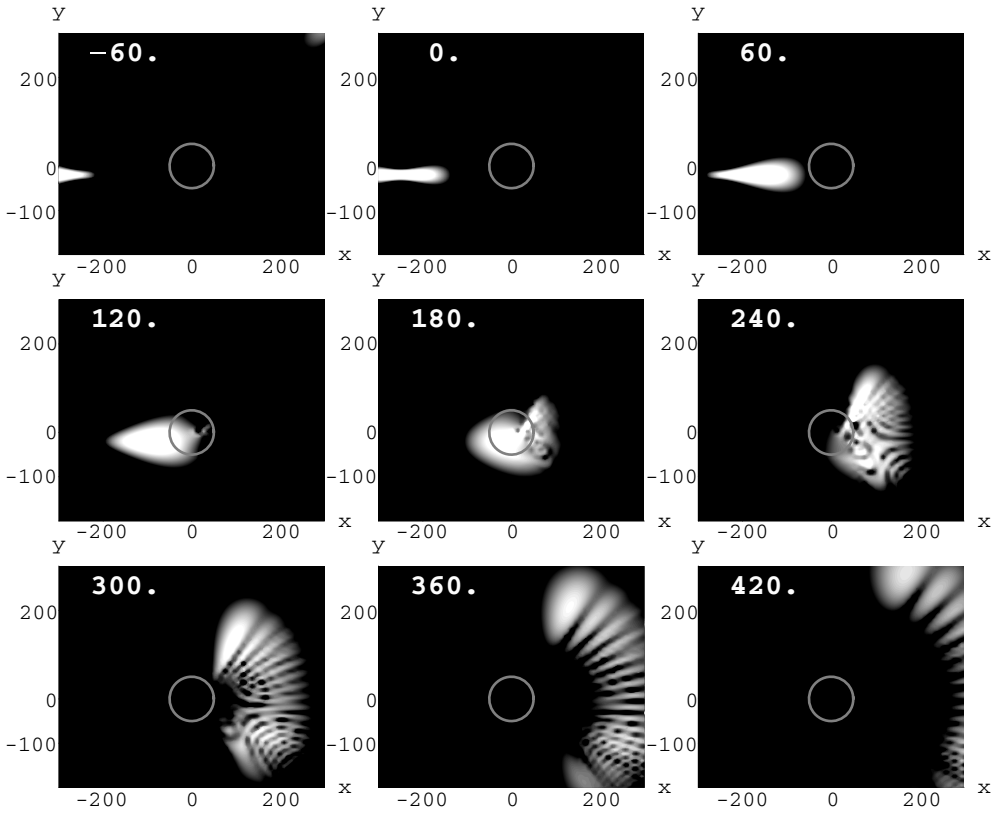

Figure 11. The same as in figure 9, with an attractive interaction, except that the initial wave packet was concentrated in the $x_0 = -250$ plane and arrived at the scatterer as a wide one, thus exhibiting wave-like or quantum features in scattering.

online journal). The pulses are composed of multi-energy stationary states. Each of those stationary states is composed of the finite transverse cross section beams described in the previous section.

Figures 9 and 10 include the displaced stationary beams concentrated inside the interaction regions that have been associated with classical orbits in the classical scattering, presented in figures 3 and 4. The discs, moving together with the wave packets, are classical particle trajectories calculated according to Newton's equation of motion. Similarities between these classical motions and the motion of the corresponding quantum wave packets determined by the Schrödinger equation are the most evident demonstration of the connection between quantum and classical mechanics.

It is important to note that this classical-like behaviour of quantum wave packets does not depend on a peculiar or precise choice of the quantum state parameters, such as $E, \Delta E, \delta E, w, x_0$ or y_0. Small changes in these parameters, in most cases, cause small changes in the corresponding wave packets, which do not alter their similarity to the classical motion.

Figures 11 and 12 show similar incident beams as in the previous cases but the beams have been concentrated in the plane at $x_0 = -250$, far before the scatterer. Approaching the scatterer, the beams have been spread to a width comparable with the interaction range and, as a result of the scattering, they have been divided into smaller diverging sub-beams. The above

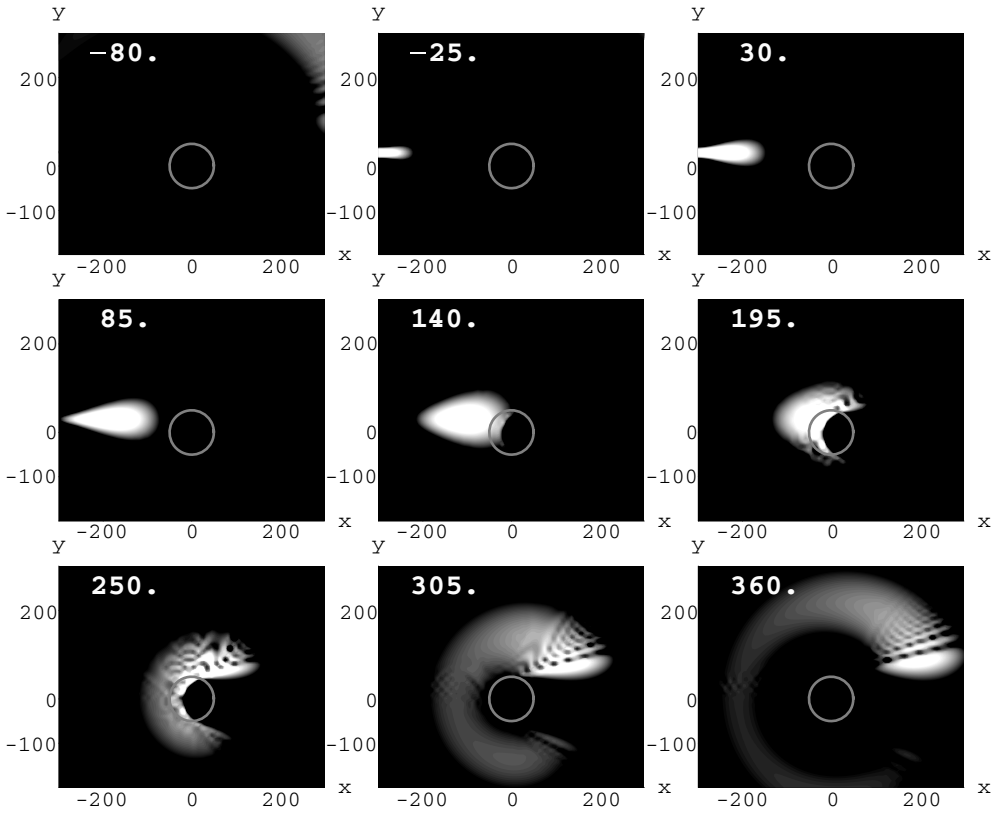

Figure 12. The same as in figure 10, with a repulsive interaction, except that the initial wave packet was concentrated in the $x_0 = -250$ plane and arrived at the scatterer as a wide one, thus exhibiting wave-like or quantum features in scattering.

division of the confined incident beam is the most characteristic feature of wave and quantum scattering.

The wave packets exhibiting classical properties cannot be confined too much, and have to remain in moderately confined states. If they were confined in too small a volume, they would spread out immediately, and in consequence, they would behave in a quantum manner.

A quantitative evaluation of the time evolution of confined nonstationary wave packets has been attempted in [10]. The accuracy of these estimations was limited and neither the wave packet spreading in free motion nor any interferences between Ψ^I and Ψ^S were described. In consequence, the scattering wavefunctions do not preserve the fixed normalization. These approximations are dramatically inconsistent in the case of confined wave packets in the interaction region (the case not considered in [10]) for which, as our discussion shows, similarities between the classical and quantum dynamics can be expected.

4. Final remarks

The present discussion emphasizes the importance of using the complete wavefunction in the description of the scattering process. This contrasts with the usual analyses which evaluate the scattering by taking into account only the scattered part of the wavefunction. In consequence

of this simplification, the resulting expressions for the differential and total scattering cross sections take the form of equations (1) and (2).

In fact, such scattering evaluations are common in most scattering theories, not only quantum, but also including scattering of electromagnetic waves by dielectric objects [2–4] and by an extended system of free electrons [5]. In these examples, the forward scattering is dominated by the interference between the scattered and incident radiation, obviously included in the total wave.

It should be noted, however, that the corrections in scattering caused by using the full wavefunction which replaces the scattered part of the wavefunction, can be insignificant. This happens if one is interested in the scattering of wide incident beams by a small scatterer (for which only a few partial waves are important) and analysing the scattering at sufficiently large distances from the scatterer. For example, in the limiting case of a point-like scatterer, for which the scattered wave has cylindrical symmetry, the discrepancies concern only the angular sector $2\pi w/r$ around the forward direction, and at a sufficient distance r the contribution of this questionable particle flux to the total scattering flux becomes negligible.

When, however, one is interested in the effect of scattering at angles overlaying the incident beam, then the use of the total wavefunction is required. In fact, Schiff [6] and Newton [8], when discussing the forward scattering and the optical theorem, recalculated the particle flux, influenced by scattering, and used the full wavefunction. As can be seen in figures 7 and 8, the forward fluxes exhibit much stronger modulations than just the magnitudes of the scattered parts $|\Psi^S|$. These point out the fact that the real modifications of the forward densities reflect not so much the amplitude of Ψ^S, but rather the amplitude of the cross product $\mathrm{Re}(\Psi^I * \Psi^S)$. It is this last factor which determines a diminution of the incident beam, for $r \to \infty$ caused by scatterers.

Throughout this paper it has been stressed several times that the individual components, Ψ^I and Ψ^S, of the total wavefunction Ψ^T are not measurable and, in consequence, not distinguishable. This statement is only valid for plain and very small detectors. However, large detectors can be composed of many parts, and can be constructed to exhibit directional sensitivity features, as is the case with, e.g., optical telescopic apparatuses. Their operation is not limited to the space outside the incident beam, and they can be immersed inside this beam. In some sense, they may play the role of collimators, as suggested by Schiff. Such instruments may be very complicated, but also a second large cylindrical scatterer, placed in the scattered field, can be of use to resolve both components Ψ^I and Ψ^S. They can be gathered into different points, as in [13], and thus independently detected. In fact, the performance of our eyes, seeing e.g. a blue sky, is connected with their vision directional sensibility.

Though these more advanced detectors can be useful when applied to large angle scatterings, they cannot resolve the scattering components scattered in the forward direction, due to their limited resolving power. In particular, if forward flux is blocked by a repulsive interaction, there will not be any scattered particle flux in the shadow sector, and the second scatter inserted there cannot provide any detectable signal.

Therefore, admitting that such direction-selective particle detectors do increase the variety of experiments and measurements, they are not useful in situations involving the moderately narrow beams for which classical-like behaviour is expected.

Our discussion indicates that classical behaviour of scattering particles can be expected when their quantum states correspond to small wave packets which remain small and undivided in passing through the strong interaction scattering region. Thus, the classical limit of a quantum system does not refer explicitly to the limit $\hbar \to 0$, usually considered as a proper condition of classical behaviour. Objections to the treatment of this limit as the classical limit of the corresponding quantum system have been raised by Wichmann [16]. He points out that

the value of $\hbar$ is associated with a system of units and ought to be fixed. Whether a particular state behaves classically or quantum mechanically should be determined by its dynamical features. The present discussion provides a quantitative confirmation of this statement.

Finally, it should be noted that although the present discussion is more specifically centred on the relation between the quantum and classical mechanics, a similar relationship exists between geometrical optics and wave optics, preliminarily presented in [17].

Appendix

In this appendix some intermediate steps illustrating the procedure of obtaining solutions of the Schrödinger equation are presented. Figure 13 shows the radial dependence of the

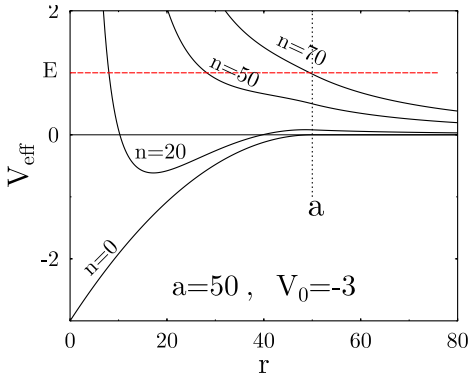

Figure 13. Radial attractive effective potentials V_{eff} for several values of the partial wave parameter n.

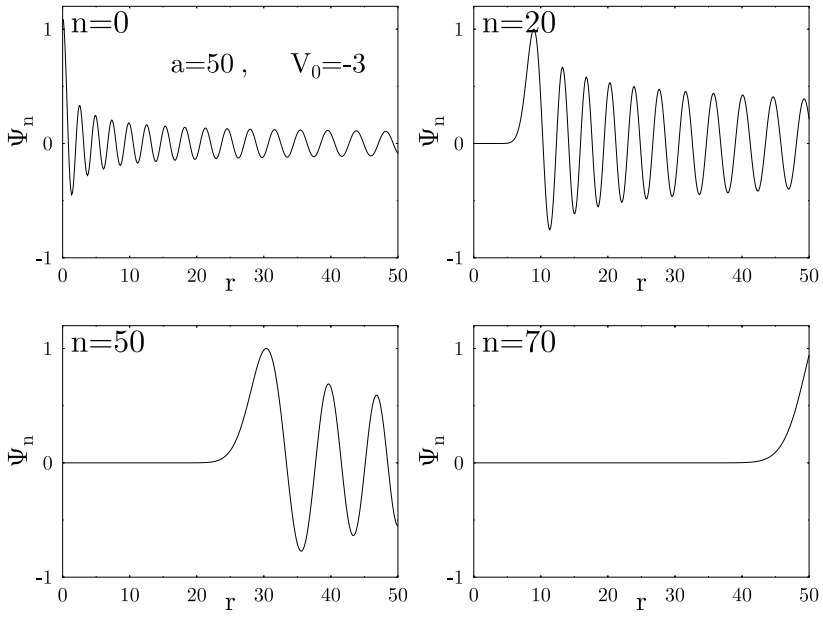

Figure 14. Internal wavefunctions ψ_{nE} for $E = 1$ and the same V_{eff} as are shown in figure 13.

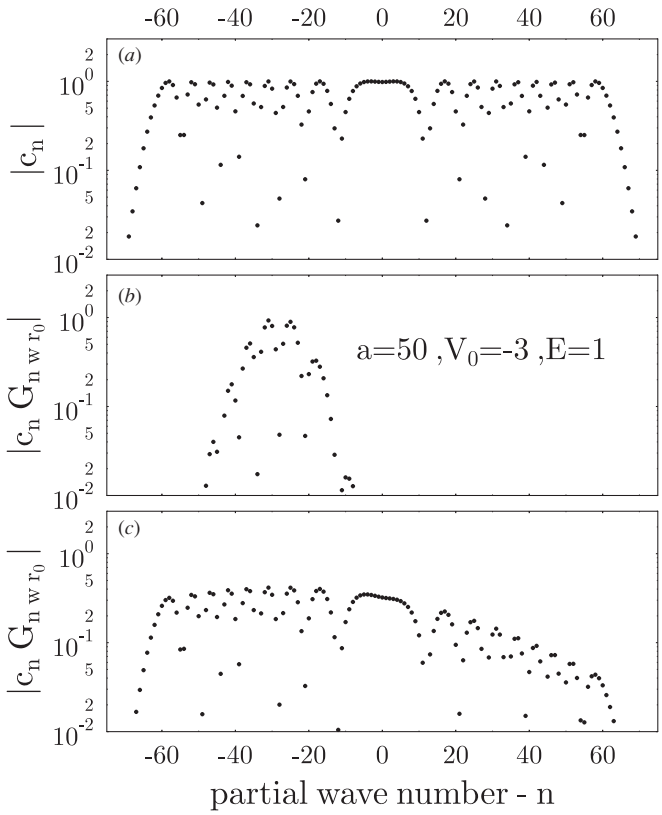

Figure 15. Magnitudes of the partial wave amplitudes for the outside atom partial wavefunctions in the cases of incident (*a*) plane wave, (*b*) narrow beam $w = 5$ shifted to $y_0 = 20$ focused inside the scatterer ($x_0 = 0$), (*c*) the above incident beam concentrated in the $x_0 = -200$ plane.

effective potential $V_{\text{eff}}(n, r) = V(r) + \frac{n^2}{2r^2}$ for several values of n in the case of an attractive interaction. Figure 14 shows the corresponding non-normalized solutions of the radial parts of the Schrödinger equation. Note how, for increasing n, these solutions are pushed out of the interaction region.

Figure 15 shows the magnitudes of the external part of the partial scattered functions for the incident plane wave (case a) and modified accordingly to the shape of the incident beam. For the narrow beam inside the interaction region only a limited range of the partial waves contributes significantly (case b). When the incident beam was concentrated far in front of the scatterer, while approaching the scatterer it widens and the number of relevant partial waves increases (case c).

References

[1] Lord Rayleigh (Strutt J W) 1945 [1878] *The Theory of Sound* vol 2 (New York: Dover) ch 18 (1st edn 1878, 2nd edn 1896)
[2] Mie G 1908 *Ann. Phys., Lpz* **25** 377
[3] Born M and Wolf E 1998 *Principles of Optics* (Cambridge: Cambridge University Press)
[4] Jackson D 1975 *Classical Electrodynamics* 2nd edn (New York: Wiley)
[5] Landau L and Lifshitz E 1959 *The Classical Theory of Fields* (London: Pergamon) ch 9–13
[6] Schiff L I 1973 *Quantum Mechanics* 3rd edn (New York: McGraw-Hill)

[7] Mott N F and Massey H S 1965 *The Theory of Atomic Collisions* (Oxford: Clarendon)
[8] Newton R G 1982 *Scattering Theory of Waves and Particles* 2nd edn (New York: McGraw-Hill)
[9] Mertzbacher E 1998 *Quantum Mechanics* 3rd edn (New York: Wiley)
[10] Joachain C J 1979 *Quantum Collision Theory* (Amsterdam: North-Holland)
[11] Amrein W O, Jauch J M and Sinha K B 1977 *Scattering Theory in Quantum Mechanics* (Reading, MA: Benjamin)
[12] Pearson D B 1988 *Quantum Scattering Theory and Spectral Theory* (London: Academic)
[13] Żakowicz W 2002 *Phys. Rev.* E **64** 066610
[14] Żakowicz W 2002 *Acta Phys. Pol.* A **101** 369
[15] Shamos M H (ed) 1987 *Great Experiments in Physics* (New York: Dover)
[16] Wichmann E H 1971 *Quantum Physics, Berkeley Physics Course* vol 4 (New York: McGraw-Hill)
[17] Żakowicz W 2002 *Acta Phys. Pol.* B **33** 2059